

Communication

Design of spectral-spatial outer volume suppression RF pulses for tissue specific metabolic characterization with hyperpolarized ^{13}C pyruvate

Albert P. Chen^{a,*}, Kevin Leung^b, Wilfred Lam^b, Ralph E. Hurd^c, Daniel B. Vigneron^d, Charles H. Cunningham^b

^a GE Healthcare, Toronto, ON, Canada

^b Sunnybrook Health Sciences Centre, Toronto, ON, Canada

^c GE Healthcare, Menlo Park, CA, United States

^d Department of Radiology and Biomedical Imaging, UCSF, San Francisco, CA, United States

ARTICLE INFO

Article history:

Received 23 March 2009

Revised 29 June 2009

Available online 3 July 2009

Keywords:

Spectral-spatial RF pulse design

Outer volume suppression

DNP

Hyperpolarized ^{13}C MR metabolic imaging

ABSTRACT

[1- ^{13}C] pyruvate pre-polarized via DNP has been used in animal models to probe changes in metabolic enzyme activities *in vivo*. To more accurately assess the metabolic state and its change from disease progression or therapy in a specific region or tissue *in vivo*, it may be desirable to separate the downstream ^{13}C metabolite signals resulting from the metabolic activity within the tissue of interest and those brought into the tissue by perfusion. In this study, a spectral-spatial saturation pulse that selectively saturates the signal from the metabolic products [1- ^{13}C] lactate and [1- ^{13}C] alanine was designed and implemented as outer volume suppression for localized MRSI acquisition. Preliminary *in vivo* results showed that the suppression pulse did not prevent the pre-polarized pyruvate from being delivered throughout the animal while it saturated the metabolites within the targeted saturation region.

© 2009 Elsevier Inc. All rights reserved.

1. Introduction

MR spectroscopy and spectroscopic imaging utilizing ^{13}C substrates hyperpolarized via DNP have been shown to provide real time *in vivo* characterization of tissue metabolism [1–5]. In one of the more promising applications of this technology, pre-polarized [1- ^{13}C] pyruvate has been used in animal models to probe changes in metabolic enzyme activities due to pathologies, apoptosis, and the physiological state of the animal. In these studies, pre-polarized [1- ^{13}C] pyruvate was injected intravenously and taken up by various tissues/organs where enzyme-facilitated reactions resulted in the observation of [1- ^{13}C] lactate, [1- ^{13}C] alanine and ^{13}C bicarbonate resonances. While many of the *in vivo* hyperpolarized ^{13}C MR studies to date have been performed with some spatial localization and different ^{13}C metabolic profiles (quantified by peak ratios or 1st order rates) have been observed in different organs/tissue types [2,6], the metabolic products observed in a particular slice/voxel are most likely a combination of local enzymatic reaction as well as perfusion.

Indeed, along with the injected pre-polarized ^{13}C substrate taken up by the tissue from the vasculature, the downstream ^{13}C metabolites produced at another site or by enzymes in the blood may also be entering the region of interest by perfusion. Thus to

more accurately assess the metabolic state and its change from disease progression or therapy in a specific region or tissue *in vivo*, it is desirable to separate the ^{13}C metabolite signals resulting from the metabolic activity within the tissue of interest and those brought into the tissue by blood.

Outer volume suppression (OVS) schemes are utilized often to provide better localization for proton MRI/MRS experiments *in vivo* [7,8]. OVS schemes usually employ a train of RF pulses prior to the imaging sequence to selectively saturate the unwanted ^1H MR signals from outside of the volume being imaged. By using a selective saturation pulse that is both spatially and spectrally selective, it may be possible to prevent polarized ^{13}C metabolites from entering the slice/voxel, while leaving the polarized ^{13}C substrate unperturbed so it can be delivered to the tissue of interest. In this study, a spectral-spatial saturation pulse that selectively saturates [1- ^{13}C] lactate and [1- ^{13}C] alanine was designed and incorporated into a double spin-echo pulse sequence. It was then tested *in vivo* in healthy rats.

2. Methods

2.1. RF pulse design

A spectral-spatial RF pulse [9–11] was designed to saturate the downstream metabolites—[1- ^{13}C] alanine and [1- ^{13}C] lactate—while leaving [1- ^{13}C] pyruvate undisturbed at 3 T. The RF

* Corresponding author. Address: GE Healthcare, 11 Brunel Court, Suite 5116, Toronto, ON, Canada M5V3Y3.

E-mail address: Albert.Chen@ge.com (A.P. Chen).

waveform was computed using the 2D SLR transform as in [10], with the VERSE algorithm applied to correct the sub-pulse shape for transmission during the gradient ramps. The RF pulse and gradient waveform are shown in Fig. 1. Spectral-spatial pulses enable the excitation (or saturation) of localized slices of magnetization within certain bands of chemical-shift, while leaving other chemical-shift species untouched. The main design consideration, and the major determinant of the duration of the pulse, was the required frequency width of the transition between saturated and un-saturated spins. This was determined by the frequency difference between pyruvate and alanine at 3 T and neutral pH: 86 Hz. This transition and the relative frequencies of the metabolites of interest can be seen in Fig. 2(a). The other design consideration was the duration of the sub-lobes, with shorter sub-lobes moving the spectral side-lobes (see arrows in Fig. 2(b)) further away from the main saturation band. Although 1 ms sub-lobes would appear to suffice based on the width of the main band, the sub-lobes were made shorter (720 μ s) to reduce the possibility of substrate saturation in the presence of main-field inhomogeneities. As demonstrated in Fig. 2(c), for a resonance in the center of the passband, only 0.01% of magnetization was consumed by each application of the pulse.

2.2. MR hardware, polarizer and compound

All *in vivo* studies were performed using a long-bore 3 T GE EXCITE™ scanner (GE Healthcare, Waukesha, WI) equipped with the MNS (multinuclear spectroscopy) hardware package. The RF coil used in the 3 T experiments was a micro-strip dual-tuned ^1H - ^{13}C rat coil (Magvale, San Francisco, CA). A HyperSense DNP polarizer (Oxford Instruments, Abingdon, UK) was used to polarize the substrate following previously described methods [12]. The preparation used in the *in vivo* experiments was a mixture of neat (99% purity) [$1\text{-}^{13}\text{C}$] pyruvic acid (Isotec, Miamisburg, OH) and 15 mM of OX063 trityl radical. The samples were polarized in a field of 3.35 T at approximately 1.4 K. Each 32 μ l [$1\text{-}^{13}\text{C}$] pyruvic acid sample was polarized for \sim 60 min prior to dissolution with \sim 5 mL of solvent consisting of 40 mM TRIS and 80 mM NaOH in distilled water, giving a nominal final pH of 7.4 [13].

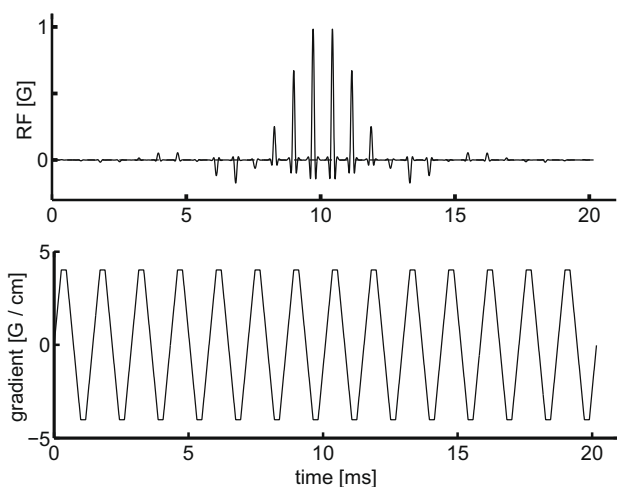


Fig. 1. Spectral-spatial RF pulse for saturating the downstream metabolites. The pulse consisted of 28 sub-lobes of 720 μ s duration, giving a net duration of 20.16 ms. The design parameters for the pulse were: spectral saturation bandwidth of 250 Hz (>99% of longitudinal magnetization saturated), spectral transition width of 125 Hz, RF sub-lobes with a time-bandwidth product of 6 (8.3 kHz bandwidth) giving a spatial transition width of 32%, 90 degree flip angle and 3.1 cm minimum slice thickness (FWHM). The gradient sub-lobes consisted of 268 μ s ramps and 184 μ s plateaus with 40 mT/m maximum amplitude. The peak RF amplitude was 0.98 G.

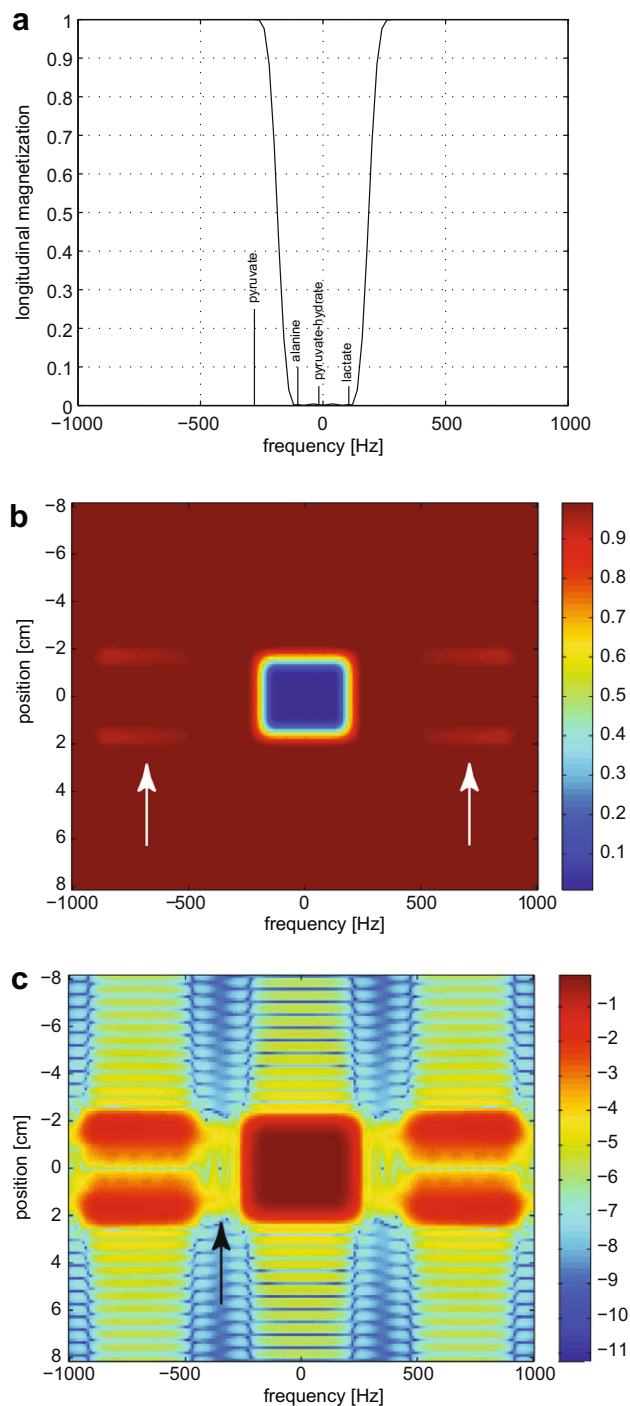


Fig. 2. Numerical simulations showing the performance of the designed spectral-spatial saturation pulse. (a) The residual longitudinal magnetization, as a function of frequency, shows the transition between saturated and un-saturated regions. (b) The spectral-spatial saturation profile shows the longitudinal magnetization after application of the pulse, where 0 indicates complete saturation and 1 indicates equilibrium magnetization. The main saturation band can be seen in the middle, with the side-lobes indicated by the white arrows. (c) By subtracting the plot in (b) from unity and taking the log base 10, the performance of the pulse in the non-saturated regions can be seen. In the un-saturated passband indicated by the black arrow, where pyruvate was placed, it is seen that only 0.01% of the magnetization was consumed by each pulse.

2.3. *In vivo* ^{13}C MRS experiments

All animal experiments followed a protocol approved by the local institutional animal research committee. Two or three hyperpo-

larized ^{13}C MRSI experiments were performed on each of the two normal male Sprague–Dawley rats included in the study. For each animal, the MRSI experiments were performed following separate (1 h apart) tail vein injections of 2.5 mL/80 mM of pre-polarized $[1-^{13}\text{C}]$ pyruvate. Care was taken to ensure the body temperature of the animal was constant throughout the imaging procedures using a heated water pad. Both the oxygen saturation and pulse rate of the animal were continuously monitored to ensure that the animals were under similar apparent physiological state for the different injections. Shim current values were kept the same throughout the experiment for a given animal.

Dynamic ^{13}C MRS data were acquired using a double spin-echo pulse sequence with a flyback echo-planar readout gradient (Fig. 3)

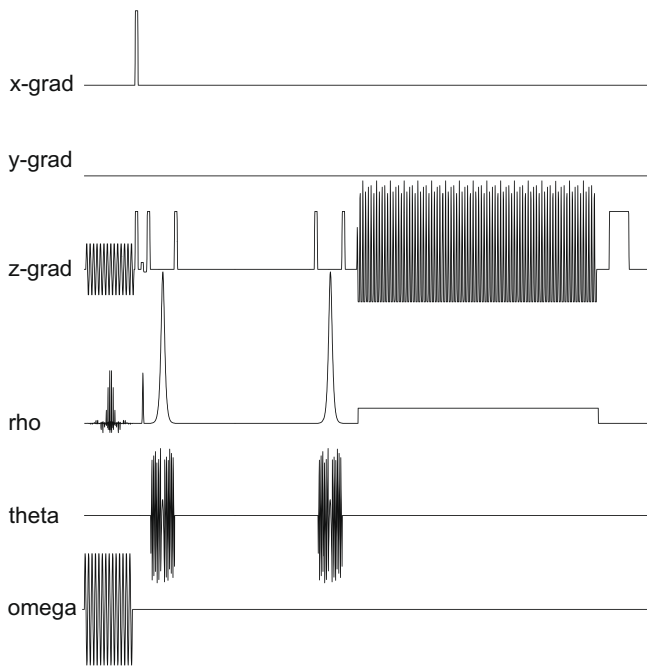


Fig. 3. Pulse sequence diagram of the double spin-echo sequence with spectral-spatial saturation and flyback echo-planar readout used in this study.

with TE of 140 ms, 5 degree excitation tip angle and the data acquisition window centered around the second spin-echo [14,15]. Adiabatic refocusing pulses were used in this double spin-echo pulse sequence, and the design and the parameters of these pulses are the same as those given in [14]. Sixty-four spectra were acquired in each experiment with 1 s temporal resolution starting 8 s after the beginning of the hyperpolarized ^{13}C pyruvate bolus injection which took ~ 10 s. One-dimensional spatial localization was performed along the z-axis using the flyback echo-planar readout gradient. Each sub-lobe of the flyback echo-planar trajectory consists of a 536 μs plateau and 624 μs of ramps ($2 * 312 \mu\text{s}$); 87 sub-lobes were used for a readout duration of 100.224 ms. Using a maximum gradient amplitude of 29.99 mT/m and readout filter of 20834 Hz/2088 pts, 12 k-space points were acquired during each plateau with 15 mm spatial resolution and 868 Hz spectral-bandwidth. No spatial localization was performed in the x and y directions [16]. For each of the animals studied, one of the ^{13}C experiments was performed with the spectral-spatial saturation pulse prior to the excitation pulse of the double spin-echo sequence (repeated for each excitation) while the other experiment(s) was performed without. The spatial saturation region was 40 mm wide, and graphically placed across the upper rat torso above the liver to cover the heart and most of the lungs of the animal (Fig. 4).

3. Results

Representative dynamic ^{13}C MRS data from a normal rat are shown in Fig. 5. The flyback echo-planar readout enabled the acquisition of data from multiple slice locations (Fig. 4, right) from a single bolus of pre-polarized $[1-^{13}\text{C}]$ pyruvate. In the experiment performed with spectral-spatial saturation, a slice that was covered by the saturation pulse containing heart and lung tissue showed no observable $[1-^{13}\text{C}]$ lactate and $[1-^{13}\text{C}]$ alanine signal but high $[1-^{13}\text{C}]$ pyruvate signal (Fig. 5, upper left). Data from the same slice in an experiment performed without the saturation pulse (upper right) demonstrated signal from both the injected substrate as well as the metabolic products. The data from a slice outside the saturation region containing rat kidneys demonstrated a normal metabolic profile [13] in both experiments with and without the saturation pulse (Fig. 5, lower left and lower right, respectively).

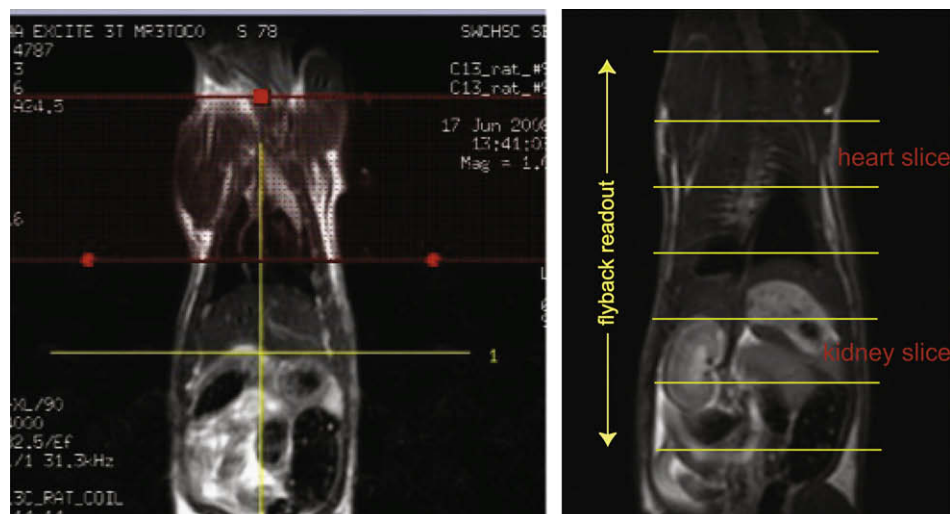


Fig. 4. T2 weighted Sagittal FSE images from one of the rat studied. The spectral-spatial band is placed across the upper torso of the animal to saturate the ^{13}C metabolite signal from the heart and lung, and the placement is performed using the interactive graphic Rx (left). The spatial localization in the dynamic MRS experiment achieved by the echo-planar readout in relation to the anatomy is also shown (right).

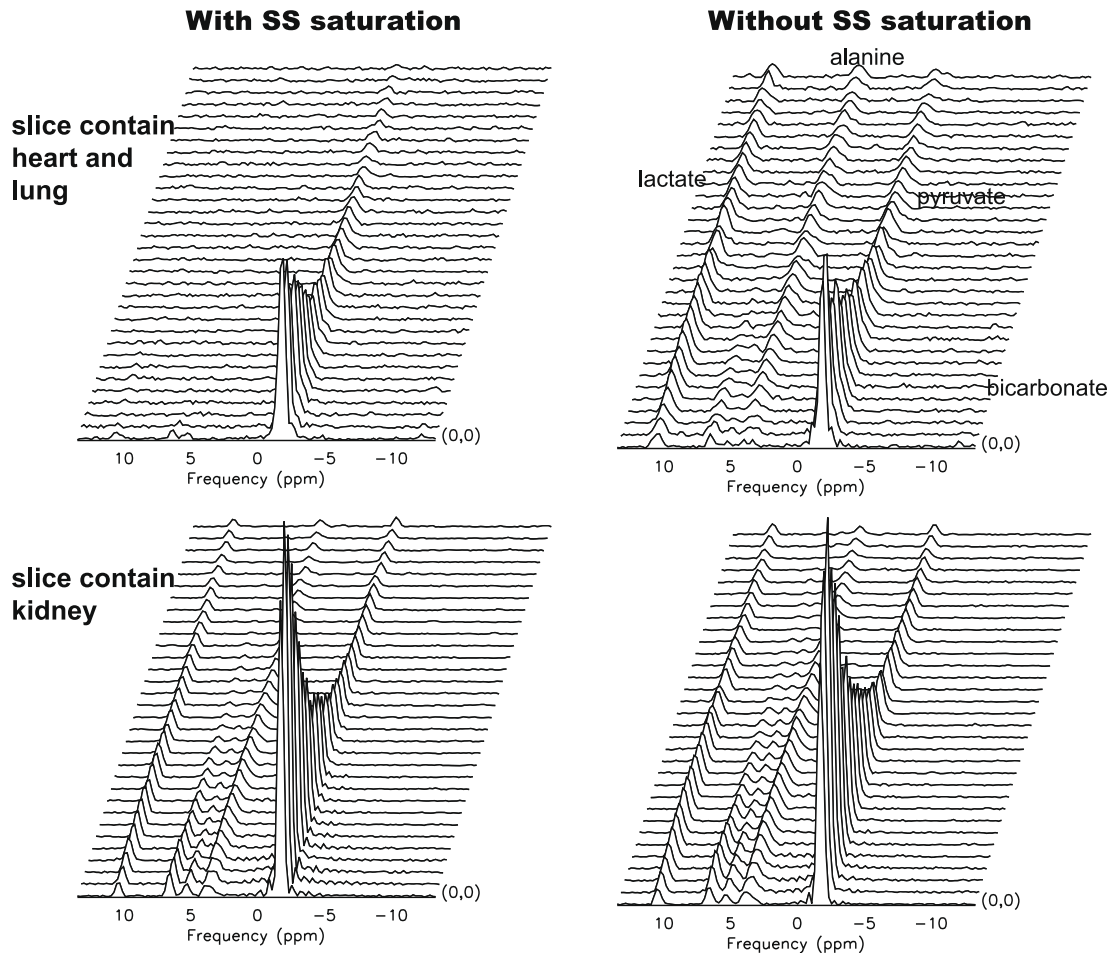


Fig. 5. Hyperpolarized ^{13}C dynamic MRS data acquired from a normal rat with (left plots) and without (right plots) spectral-spatial saturation pulse. Data from a slice containing heart and lung (upper plots) and a slice containing kidney (lower plots) are shown. ^{13}C metabolites lactate and alanine were clearly saturated in the heart/lung slice in the experiment with SS saturation pulse, while the data seemed to be similar in the kidney slice with or without the SS saturation pulse.

Fig. 6 shows normalized lactate peak amplitude vs time in the kidney slice from three experiments performed in the other normal rat. Two of the experiments were performed with spectral-spatial saturation over the rat heart/lung and the other was performed without saturation. The lactate peak amplitudes were normalized

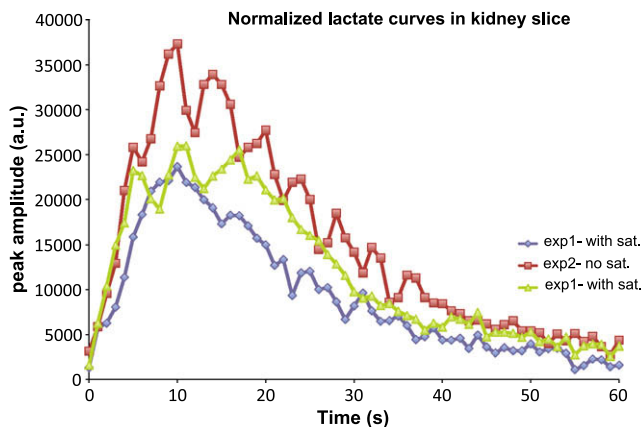


Fig. 6. ^{13}C Lactate peak amplitude time course data from the kidney slice of a normal rat. In three experiments performed, two datasets were acquired with spectral-spatial saturation over the upper torso of the animal and the other dataset was acquired with saturation. Lactate data was normalized by the total pyruvate signal from the same slice and the same experiment. Lower lactate signal was observed in experiments with saturation.

by total pyruvate signal from the same slice of that particular experiment. While the shape of the lactate curves were the same for the three experiments, lower peak ^{13}C lactate signal was observed in the two experiments performed with saturation as compared to the experiment performed without. For the two animals studied (five datasets), the peak lactate signals without saturation was higher in both animals and on average 1.34 ± 0.24 times the signal with saturation ($p = 0.052$, by paired t -test).

4. Discussion

A spectral-spatial saturation pulse was designed to selectively saturate both $[1-^{13}\text{C}]$ lactate and $[1-^{13}\text{C}]$ alanine 3 T. The hypothesis was that the pool of substrate not initially taken up by the tissue of interest will be metabolized at other sites and may enter the tissue of interest via perfusion. Thus the total ^{13}C metabolite (such as $[1-^{13}\text{C}]$ lactate) signal observed in a slice or voxel may include metabolites resulting from local enzyme-mediated exchange as well as metabolites arriving through the blood. By eliminating the metabolite signals circulating through the heart, this second source of metabolite signal would be reduced. The observations reported in this study support this hypothesis.

To allow the resonances outside this chemical-shift range to be completely un-perturbed, the side-lobes (Fig. 2, lower graph, arrows) that are an unavoidable part of the spectral-spatial design need to be carefully considered, especially if the pulse is applied in

regions where susceptibility induced shifts and large spectral line-widths may be expected (such as cardiac applications). Thus in the current design the side-lobes were moved as far away as was feasible with the desired spatial width to ensure that the substrate passes through the pulse unaffected. Design enhancements such as a “fly-back” gradient trajectory to limit the sensitivity to gradient eddy currents, and oscillating RF sub-lobe polarity to increase the width of the stop band [10,11] were considered but did not offer any improvement. A flyback design, in which RF is only transmitted on the positive gradient sub-lobes, would increase the peak B1 amplitude, which at 0.98 G (Fig. 1.) is already near the maximum achievable with the RF coil used in the experiments. The use of oscillating RF sub-lobe polarity did not offer an advantage because the unwanted saturation in the passband (0.01%) was due to the ripples emanating from the passband so that suppressing one of the sidelobes would not improve this performance measure. However, in applications that the chemical shifts between the injected ^{13}C substrate and metabolic products are much larger, this design may have to be considered. Furthermore, a shorter pulse duration, which would normally be enabled by suppressing one of the sidelobes, would not be possible in this case because the spectral transition width between the stopband and the passband was already at the limit with the current pulse duration.

In the data acquired from a slice containing rat heart and lung tissue with and without the spectral-spatial saturation pulse placed in the same spatial region (Fig. 5, upper plots), the $[1-^{13}\text{C}]$ pyruvate signal did not appear to have been affected, with the difference in peak pyruvate SNR between the two acquisitions less than 1%. In the data acquired from the other animal, pyruvate peak SNR in the similar slice was actually 10% higher for the studies with the saturation pulse, although substrate polarization was not measured in these studies. Nonetheless, in these preliminary studies, the hyperpolarized substrate was not negatively impacted by the use of the saturation pulse. It is also worth noting that ^{13}C bicarbonate signal was indeed detected in the experiments with the saturation pulse, since ^{13}C bicarbonate resonance was not in the spectral saturation region of this pulse.

Data from a slice through the rat kidney acquired with and without the spectral-spatial saturation pulse had almost identical appearance (Fig. 5, lower plots). High signal from the injected substrate $[1-^{13}\text{C}]$ pyruvate was observed initially, which then decayed over time by both T1 relaxation as well as the exchange of the ^{13}C label between the substrate and the metabolites $[1-^{13}\text{C}]$ lactate and $[1-^{13}\text{C}]$ alanine. However, when the metabolite signal (in this case, lactate) was normalized by the substrate signal in the slice, there was a notable difference between the experiments performed with and without the spectral-spatial pulse (Fig. 6). In this animal study, the two experiments with saturation pulse were performed before and after the experiment without saturation pulse and they demonstrated very similar results (lower lactate). Thus it is unlikely that the differences observed were due to any physiological changes of this animal throughout the study.

Since the saturation pulse was designed as a spectral-spatial pulse and can be graphically prescribed, it would be feasible to use multiple bands to contour a particular region of interest such as a tumor. By doing so in conjunction with a MRS/MRSI acquisition following the injection of a pre-polarized, metabolically active substrate, it may be possible to probe more directly the enzyme activity in that particular tissue without influence from perfusion. The specificity of hyperpolarized ^{13}C MR MRS/MRSI for characterizing changes in metabolic profile due to pathology or treatment may then be increased.

5. Conclusion

A design of a spectral-spatial saturation pulse to eliminate unwanted metabolite signals for ^{13}C MRS/MRSI studies utilizing pre-polarized $[1-^{13}\text{C}]$ pyruvate was demonstrated. Preliminary *in vivo* results showed that the saturation pulse did not prevent the substrate from being delivered throughout the animal while it saturated the metabolites within the targeted region. Reduced $[1-^{13}\text{C}]$ lactate signal was observed in data obtained from a slice through the rat kidney in experiments where the saturation pulse was placed over the heart/lung of the animal as compared with control experiments.

Acknowledgments

This work was supported by the Canadian Institutes of Health Research, the Ontario Institute for Cancer Research, the McLaughlin Centre for Molecular Medicine and NIH RO1 EB007588.

References

- [1] K. Golman, R. Zandt, M. Thaning, Real-time metabolic imaging, *PNAS* 103 (30) (2006) 11270–11275.
- [2] S.E. Day, M.I. Kettunen, F.A. Gallagher, D. Hu, M. Lerche, J. Wolber, K. Golman, J.H. Ardenkjaer-Larsen, K.M. Brindle, Detecting tumor response to treatment using hyperpolarized ^{13}C magnetic resonance imaging and spectroscopy, *Nat. Med.* 13 (11) (2007) 1382–1387.
- [3] M. Albers, R. Bok, A.P. Chen, C.H. Cunningham, M.L. Zierhut, V.Y. Zhang, S.J. Kohler, J. Tropp, R.E. Hurd, Y. Yen, S.J. Nelson, D.B. Vigneron, J. Kurhanewicz, Hyperpolarized ^{13}C lactate, pyruvate, and alanine: noninvasive biomarkers for prostate cancer detection and grading, *Cancer Res.* 68 (20) (2007) 8607–8615.
- [4] M.A. Schroeder, L.E. Cochlin, L.C. Heather, K. Clark, G.K. Radda, D.J. Tyler, *In vivo* assessment of pyruvate dehydrogenase flux in the heart using hyperpolarized carbon-13 magnetic resonance, *PNAS* 105 (33) (2008) 12051–12056.
- [5] M.E. Merritt, C. Harrison, C. Storey, F.M. Jeffrey, A.D. Sherry, C.R. Malloy, Hyperpolarized ^{13}C allows a direct measure of flux through a single enzyme-catalyzed step by NMR, *PNAS* 104 (50) (2007) 19773–19777.
- [6] A.P. Chen, P. Albers, C.H. Cunningham, S.J. Kohler, Y. Yen, R.E. Hurd, J. Tropp, R. Bok, S.J. Nelson, J. Kurhanewicz, D.B. Vigneron, Hyperpolarized C-13 spectroscopic imaging of the TRAMP mouse at 3T-Initial experience, *Magn. Reson. Med.* 58 (6) (2007) 1099–1106.
- [7] P. Le Roux, R.J. Gilles, G.C. McKinnon, P.G. Carlier, Optimized outer volume suppression for single-shot fast spin-echo cardiac imaging, *J. Magn. Reson. Imaging* 8 (5) (1998) 1022–1032.
- [8] T.K. Tran, D.B. Vigneron, N. Sailasuta, J. Tropp, P. Le Roux, J. Kurhanewicz, S. Nelson, R. Hurd, Very selective suppression pulses for clinical MRSI studies of brain and prostate cancer, *Magn. Reson. Med.* 43 (1) (2000) 23–33.
- [9] C.H. Meyer, J.M. Pauly, A. Macovski, D.G. Nishimura, Simultaneous spatial and spectral selective excitation, *Magn. Reson. Med.* 15 (2) (1990) 287–304.
- [10] J. Pauly, D. Spielman, A. Macovski, Echo-planar spin-echo and inversion pulses, *Magn. Reson. Med.* 29 (6) (1993) 776–782.
- [11] Y. Zur, Design of improved spectral-spatial pulses for routine clinical use, *Magn. Reson. Med.* 43 (3) (2000) 410–420.
- [12] J.H. Ardenkjaer-Larsen, B. Fridlund, A. Gram, G. Hansson, L. Hansson, M.H. Lerche, R. Servin, M. Thaning, K. Golman, Increase in signal-to-noise ratio of > 10,000 times in liquid-state NMR, *Proc. Natl. Acad. Sci. USA* 100 (18) (2003) 10158–10163.
- [13] S.J. Kohler, Y. Yen, J. Wolber, A.P. Chen, M.J. Albers, R. Bok, V. Zhang, J. Tropp, S. Nelson, D.B. Vigneron, J. Kurhanewicz, R.E. Hurd, *In vivo* ^{13}C carbon metabolic imaging at 3T with hyperpolarized ^{13}C -1-pyruvate, *Magn. Reson. Med.* 58 (1) (2007) 65–69.
- [14] C.H. Cunningham, A.P. Chen, M.J. Albers, J. Kurhanewicz, R.E. Hurd, Y. Yen, S.J. Nelson, D.B. Vigneron, Double spin-echo sequence for rapid spectroscopic imaging of hyperpolarized ^{13}C , *J. Magn. Reson.* 287 (2) (2007) 357–362.
- [15] A.P. Chen, R.E. Hurd, C.H. Cunningham, M. Albers, M.L. Zierhut, Y.F. Yen, J. Tropp, R. Bok, S.J. Nelson, J. Kurhanewicz, D.B. Vigneron, Symmetric Echo Acquisition of Hyperpolarized C-13 MRSI Data in the TRAMP Mouse at 3T, ISMRM 15th annual meeting, Berlin, Germany, 2007, p. 538.
- [16] C. Cunningham, D. Vigneron, A. Chen, D. Xu, S. Nelson, R. Hurd, D. Kelley, J. Pauly, Design of flyback echo-planar readout gradients for magnetic resonance spectroscopic imaging, *Magn. Reson. Med.* 54 (2005) 1286–1289.